Th17 Cells Exhibit a Distinct Calcium Profile from Th1 and Th2 Cells and Have Th1-Like Motility and NF-AT Nuclear Localization[1]

K. Scott Weber, Mark J. Miller, and Paul M. Allen[2]

Helper T cell subsets have evolved to respond to different pathogens, and upon activation secrete distinct sets of cytokines. The discovery and identification of Th17 cells, which develop via a unique lineage from Th1 and Th2 cells, have provided new insights into aspects of immune regulation and host defense that were previously unclear. A key early signaling event upon Ag recognition is elevation of intracellular free Ca^{2+}, and cytokine expression can be differentially induced depending on the duration, amplitude, and pattern of Ca^{2+} signaling. Th1 and Th2 cells can be distinguished by their Ca^{2+} profiles, and we provide in this study the first report regarding Ca^{2+} signaling in Th17 cells. Th17 cells have a distinct Ca^{2+} signaling profile from Th1 and Th2 cells with intermediate sustained Ca^{2+} levels and increased oscillations compared with Th2 cells. Elevated intracellular Ca^{2+} has been shown to inhibit T cell motility, and we observed that Th17 cells, like Th1 cells, are less motile than Th2 cells. Analysis of NF-AT nuclear localization revealed that Th1 and Th17 cells have significantly higher levels at later time points compared with Th2 cells. Thus, these findings show that Th17 cells, in addition to their distinct cytokine response from Th1 and Th2 cells, display unique patterns of intracellular Ca^{2+} signaling and Th1-like motility behavior and nuclear localization of NF-AT. *The Journal of Immunology,* **2008, 180: 1442–1450.**

T helper cells have historically been characterized into two subsets, Th1 and Th2 cells, based upon distinct cytokine secretion patterns in response to Ag stimulation. Th1 cells drive cell-mediated immunity and have evolved to respond to intracellular pathogens, whereas Th2 cells promote Ab-mediated immunity and aid in the clearance of parasites (1–6). The discovery of an IL-17-producing subset of $CD4^+$ T cells in the inflamed joints of Lyme disease patients provided evidence for a potential new helper subtype (7, 8). Identification of IL-6 and TGF-β as the key factors for naive T cell differentiation to Th17 cells has permitted examination of their roles in immune regulation and host defense (9, 10). Characterization of these Th17 cells, which develop via a unique lineage from Th1 and Th2 cells, has led to a revision of the Th1-Th2 paradigm (11–15).

Th17 cells act as a distinct effector subset and secrete the signature cytokine IL-17, a proinflammatory cytokine that recruits and activates neutrophils, enhances T cell priming, and promotes the release of inflammatory mediators. Th17 cells provide defense against extracellular bacteria, mediate inflammation, and are critical for many types of autoinflammatory disorders (i.e., experimental autoimmune encephalomyelitis, type II collagen-induced arthritis, inflammatory bowel disease, and psoriasis) (15–21). The discovery and initial characterization of these Th17 cells have provided a potential explanation for various chronic disease pathologies that were unclear with an understanding of only the Th1 and Th2 cell subsets (14, 22–24). Studies examining the signaling pathways of Th17 cells have just begun, and to date no studies have examined Th17 calcium signaling.

Calcium signaling permits the transcription of genes essential for T cell effector functions (i.e., cytokines) and is also important for numerous other functions, including proper thymic selection, growth, differentiation, and death of T cells (25–30). T cell recognition of foreign Ag initiates a cascade of signaling events that results in an increase in intracellular free calcium ($[Ca^{2+}]_i$),[3] and the amplitude, duration, and kinetics of the $[Ca^{2+}]_i$ signal have been shown to alter the efficiency and specificity of downstream transcription factors and gene expression (29–31). Previous work from our laboratory and others has shown that Th1 and Th2 cells have distinct $[Ca^{2+}]_i$ patterns after stimulation by Ag (32–34). Th1 cells reach high concentrations of $[Ca^{2+}]_i$ and then oscillate from low to high $[Ca^{2+}]_i$ levels numerous times. Th2 cells also initially reach high concentrations of $[Ca^{2+}]_i$, but then return close to baseline levels with few oscillations (34). Furthermore, $[Ca^{2+}]_i$ signaling has been shown to play an important role in lymphocyte motility, with studies examining cellular motility both in vitro and in vivo revealing that elevated levels of $[Ca^{2+}]_i$ correlate with inhibited T cell motility (31, 35–37). T cell movement within secondary lymphoid tissue is important in determining the fate of T cell interactions with APCs, where T cells will traffic, the type of Ag-specific help they can provide, and the cells eventually involved in an immune response (38).

In this study, we describe the Th17 $[Ca^{2+}]_i$ profile that is distinct from Th1 and Th2 cells. After Ag stimulation, Th17 cells maintain intermediate sustained $[Ca^{2+}]_i$ levels, higher than Th2

Department of Pathology and Immunology, Washington University School of Medicine, St. Louis, MO 63110

Received for publication April 30, 2007. Accepted for publication November 28, 2007.

The costs of publication of this article were defrayed in part by the payment of page charges. This article must therefore be hereby marked *advertisement* in accordance with 18 U.S.C. Section 1734 solely to indicate this fact.

[1] This work was supported by grants from the National Institutes of Health, and K.S.W. was supported by a National Institutes of Health training grant.

[2] Address correspondence and reprint requests to Dr. Paul M. Allen, Washington University School of Medicine, Department of Pathology and Immunology, 660 South Euclid Avenue, Campus Box 8118, St. Louis, MO 63110. E-mail address: pallen@wustl.edu

[3] Abbreviations used in this paper: $[Ca^{2+}]_i$, intracellular free calcium; PLCγ1, phospholipase Cγ1; Hb, hemoglobin.

cells and lower $[Ca^{2+}]_i$ levels than Th1 cells. Additionally, Th17 cell $[Ca^{2+}]_i$ oscillations are similar to Th1 cells, and both are significantly greater than Th2 cells. Elevated $[Ca^{2+}]_i$ levels have been shown to inhibit T cell motility, and we found that Th1 and Th17 cells are both significantly less motile than Th2 cells. Analysis of NF-AT nuclear localization revealed that Th1 and Th17 cells had significantly higher levels of localization compared with Th2 cells at later time points. Collectively, our data provide the first characterization of the $[Ca^{2+}]_i$ signaling pattern, motility, and NF-AT localization of the recently identified Th17 cells in comparison with Th1 and Th2 cells.

Materials and Methods

T cell isolation and maintenance

The 2.102 TCR-transgenic mouse was generated and bred to RAG1-deficient mice, as published previously (39). Primary 2.102 T cells were isolated from the spleens of 2.102 TCR-transgenic mice, and $CD4^+$ T cells were enriched using magnetic cell sorting (Miltenyi Biotec). CBA/J mice were purchased from The Jackson Laboratory, and spleen cells, containing the Hbb^d epitope that stimulates 2.102 cells, were isolated and irradiated (3000 rad) for use as APCs. All mice used in this study were between 5 and 10 wk of age. The 2.102 T cells (1×10^6) and irradiated CBA/J spleen cells (5×10^6) were added to a 12-well cell culture plate with the addition of the T cell-specific cytokines and Abs described below. Primary T cells were cultivated in medium containing IMDM supplemented with 2 mM GlutaMAX (Invitrogen Life Technologies), 5×10^{-5} M 2-ME, and 50 μg/ml gentamicin.

T cell polarization

T cells were polarized to Th1, Th2, or Th17 subtypes in vitro by the addition of the following: 1) 10 ng/ml IL-12 (R&D Systems) and 10 μg/ml anti-IL-4 mAb (clone 11B11) for Th1 cell polarization; 2) 10 ng/ml IL-4 (R&D Systems) and 10 μg/ml anti-IL-12 mAb (clone TOSH) for Th2 cell polarization; and 3) 20 ng/ml IL-6 (R&D Systems) and 3 ng/ml TGF-β1 (R&D Systems), along with 10 μg/ml each of anti-IFN-γ (clone H22), anti-IL-12, and anti-IL-4 mAbs for Th17 cell polarization. IL-2 (100 U) was added to the medium 48 h after initial stimulation, and T cell cultures were split 1:2. Cells were restimulated after 7 days in culture, and the same cytokines and Abs described above were added again. The polarized T cells were used on day 14.

Intracellular cytokine staining

Th cells were stimulated with 50 ng/ml PMA and 500 ng/ml ionomycin and incubated for 5 h at 37°C; brefeldin A (10 μg/ml) was added for the last 3 h of the incubation. The cells were fixed in 2% paraformaldehyde for 20 min at room temperature, and then washed and permeabilized with 0.5% saponin for 10 min. Intracellular staining was performed for 30 min at room temperature using FITC-conjugated anti-IFN-γ (BD Biosciences), PE-conjugated anti-IL-4 (BD Biosciences), or PE-conjugated anti-IL-17 (BD Biosciences). CellQuest software and a FACScan (BD Biosciences) were used for data collection and analysis.

Calcium imaging

Immediately before use, polarized T cells were incubated with 1 μM fura 2-AM (Molecular Probes) for 30 min at 37°C in Ringers imaging solution (150 mM NaCl, 10 mM glucose, 5 mM HEPES, 5 mM KCl, 1 mM $MgCl_2$, and 2 mM $CaCl_2$), washed, and then incubated in Ringers solution for another 30 min at 37°C. After washing, 100,000 fura 2-loaded T cells were pipetted onto 100,000 adherent APCs ($Hi7\text{-}E^k$) that had been loaded with 1 μM hemoglobin (Hb) (64–76) overnight. The Hb (64–76) peptide was synthesized using standard Fmoc chemistry, purified by reverse-phase HPLC, and confirmed using MALDI mass spectrometry, as has been previously described (40). The location of the APCs and T cells was monitored by visualizing the cells with transmitted light every 3 s. All imaging was done in 8-chamber coverglass slides (Lab-Tek, Nalge Nunc International).

Calcium imaging was performed at 37°C using a temperature-controlled environmental chamber on a Zeiss axiovert 200M microscope equipped with a xenon arc lamp. Fura 2-loaded cells were excited using 340 and 380 excitation filters (71000a set; Chroma Technology) and a polychroic mirror (73100bs; Chroma Technology). Fluorescence was passed through a 510 ± 40 wide band emission filter (Chroma Technology) and captured by a Cascade 512B camera (Roper Scientific). Ratio measurements (340/380) were recorded at 3-s intervals over a 50-min time period. The $[Ca^{2+}]_i$ concentration was estimated by determining the minimal (R_{min}) and maximal (R_{max}) fluorescence by exposing T cells to a Ca^{2+}-free solution containing 10 μM ionomycin and 4 mM EGTA or a solution containing 10 mM Ca^{2+} and 10 μM ionomycin. These values were then used in the Grynkiewicz equation (41), as follows: $[Ca^{2+}]_i = K_d \times S_f\ [(R - R_{min})/(R_{max} - R)]$, where K_d was assumed to be 260 nM, and S_f was the 380 nm ratio of the observed emission intensity of Ca^{2+}-free to Ca^{2+}-saturated conditions.

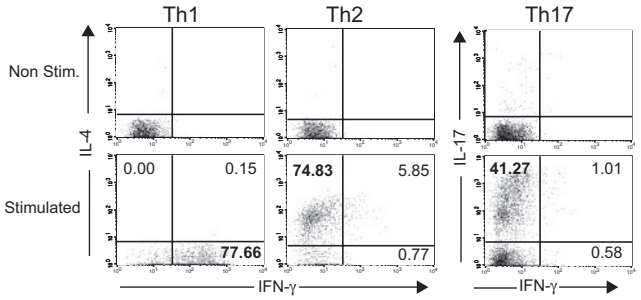

FIGURE 1. Intracellular cytokine staining of polarized Th1, Th2, and Th17 cells. T cell subtypes were polarized, as described in *Materials and Methods*. Histograms show intracellular staining for Th1 cells (IFN-γ and IL-4), Th2 cells (IFN-γ and IL-4), and Th17 cells (IL-17 and IFN-γ). The polarized cells (day 14) were stimulated with PMA and ionomycin for 5 h, with the addition of brefeldin A the final 3 h. Cells from the lymphocyte gate were used for analysis, and numbers in quadrants indicate the frequency of cells staining positive for the cytokines. In this representative experiment, 77.66% of Th1 cells were IFN-γ positive, 74.83% of Th2 cells were IL-4 positive, and 41.27% of Th17 cells were IL-17 positive.

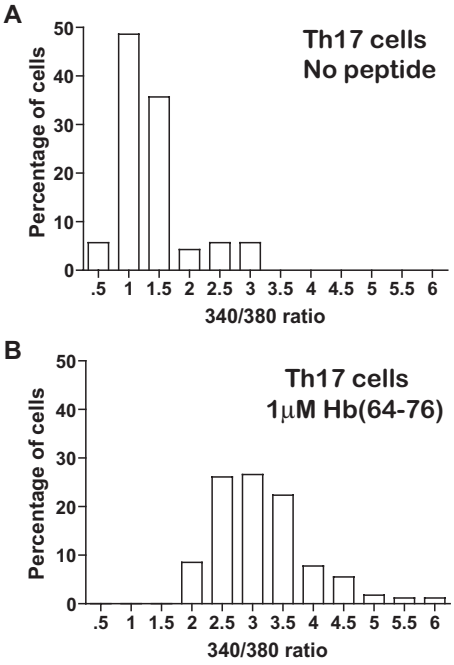

FIGURE 2. Calcium response of Th17 cells without and with Hb (64–76) peptide. *A*, Th17 cell calcium response to DCEK/ICAM APCs without the addition of any peptide. Histogram shows the plateau 340/380 ratio of each T cell in the field after 10 min. The percentage of T cells is shown at each ratio, and the total number of T cells counted was 70. *B*, Th17 cell calcium response to DCEK/ICAM APCs ($Hi7\text{-}E^k$) that had been pulsed with 1 μM Hb (64–76) peptide overnight. Histogram shows the plateau 340/380 ratio of each T cell in the field after 10 min. The percentage of T cells is shown at each ratio, and the total number of T cells counted was 165.

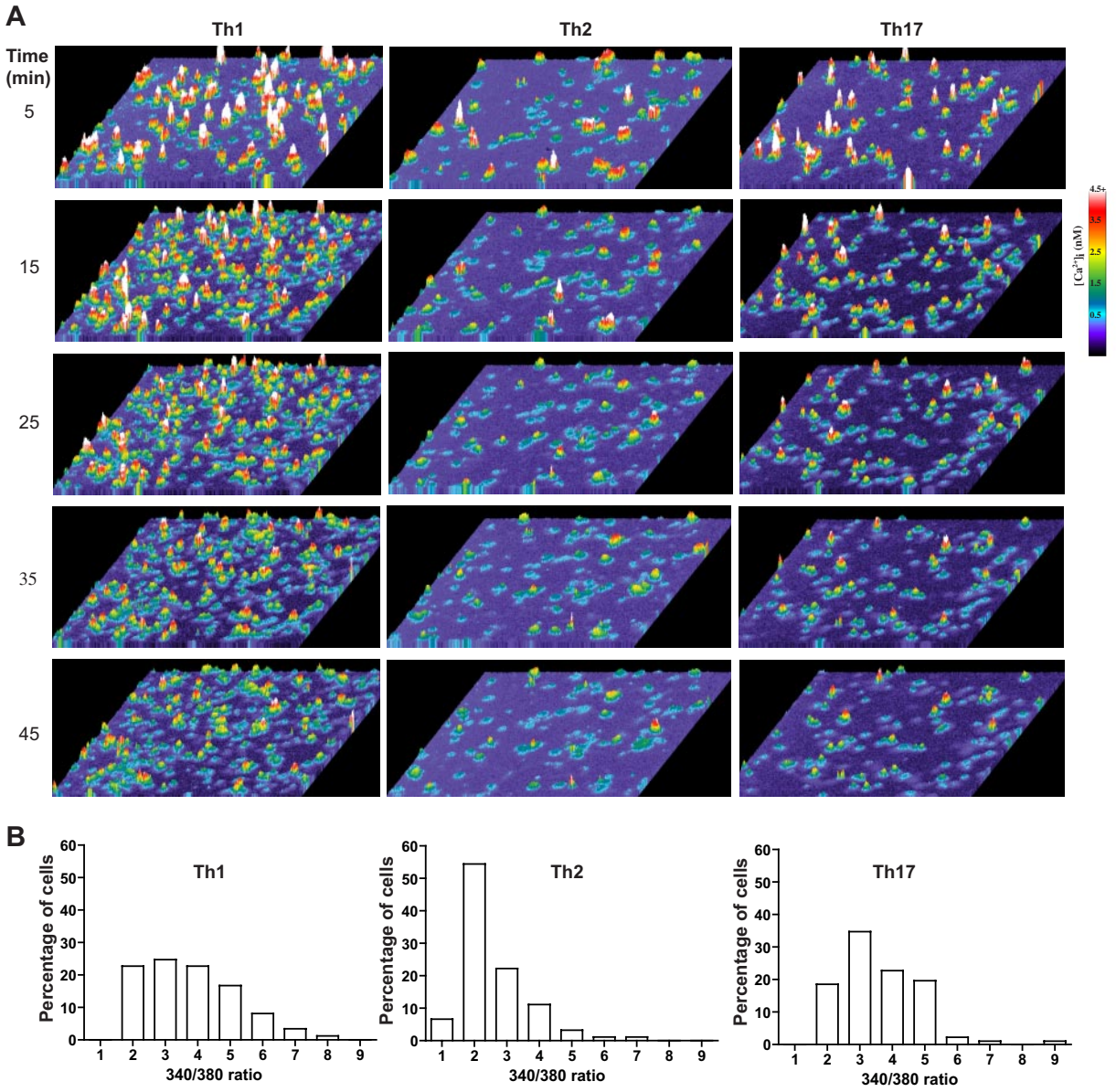

FIGURE 3. Snapshots showing Th1, Th2, and Th17 cell calcium mobilization and plateau histograms. *A*, Snapshots of Th1, Th2, and Th17 $[Ca^{2+}]_i$ intensity profiles at 5-, 15-, 25-, 35-, and 45-min time points. APCs (Hi-7 E^k cells) were pulsed with 1 μM Hb (64–76) peptide overnight, and equal numbers of T cells were added to each well at time 0. The snapshots show the $[Ca^{2+}]_i$ ratio images obtained with fura 2 (340/380-nm excitations). Relative $[Ca^{2+}]_i$ levels (340/380 ratios) are compared using a pseudocolor scale, as indicated by the scale bar on the *left* (i.e., white is a ratio >4.5, red is ~3.5, etc.). *B*, Histograms showing the plateau $[Ca^{2+}]_i$ levels for Th1, Th2, and Th17 cells as measured by 340/380 ratios. The histograms display the percentage of cells and corresponding 340/380 levels 5 min after the T cells were introduced to Ag (149 Th1 cells, 90 Th2 cells, and 92 Th17 cells). Th2 cells are more common at the lower $[Ca^{2+}]_i$ levels (mean ± SEM = 3.064 ± 0.1146) than Th1 cells (4.268 ± 0.1165), and their differences in mean values are statistically significant ($p < 0.05$). Th17 cell $[Ca^{2+}]_i$ levels (4.066 ± 0.1363) are also significantly higher ($p < 0.05$) than Th2 cells and have a similar mean and distribution as Th1 cells.

Naive T cell isolation

The 2.102 splenic $CD4^+$ T cells were enriched by staining with Miltenyi CD4 beads and separated using LS columns, according to the manufacturer's specifications (Miltenyi Biotec). The enriched $CD4^+$ T cells were stained with anti-CD4 allophycocyanin (Biolegend), anti-CD62L FITC (BD Biosciences), and anti-CD44 PE (Biolegend) for 1 h on ice, washed, and sort purified by gating on the $CD4^+$, $CD62L^{high}$, $CD44^{low}$ population.

Western blots

T cells were stimulated by Hi7 cells (1 μM Hb (64–76)) for 0, 5, 15, or 25 min and lysed in 2× Laemmli sample buffer (Sigma-Aldrich). The lysates were boiled for 5 min at 100°C, resolved on a 10% SDS-PAGE gel (~5×10^6 cells/sample), and transferred onto a nitrocellulose membrane (Bio-Rad). The blots were blocked with 1:1 PBS:blocking buffer (LI-COR) for 1 h and probed (1:1000 in PBS-T) with primary Abs (rabbit anti-phospho-phospholipase Cγ1 (PLC)γ1, Cell Signaling Technology; or mouse anti-PLCγ1, Upstate Biotechnology) overnight at 4°C. The membranes were probed (1:200 in PBS-T + SDS) with secondary Abs (goat anti-rabbit 680 or goat anti-mouse 800; LI-COR) for 1 h at room temperature. Bands were visualized and quantified with the Odyssey infared imaging system (LI-COR).

Nuclear localization

A total of 2×10^5 T cells/sample was stimulated by Hi7 cells (1 μM Hb (64–76)) for 0, 5, 15, or 45 min at 37°C in 8-chamber coverglass slides (Lab-Tek, Nalge Nunc International). Stimulation was stopped by the addition of 200 μl of ice-cold PBS. Cells were fixed with 100 μl of BD Cytofix (BD Biosciences) for 20 min at room temperature and washed

twice with PBS. Cells were blocked and permeabilized in a permeabilization buffer (.5% saponin and 1% BSA) for 10 min at room temperature. Cells were stained (1:100) for 1 h at room temperature in 100 μl of permeabilization buffer with the NF-ATc1 primary Ab (7A6; Santa Cruz Biotechnology), washed, and stained (1:200) in 100 μl of permeabilization buffer with the secondary Ab (goat anti-mouse Alexa Fluor 546; Molecular Probes). Cells were washed and incubated with 1 μM SYTO13 (Molecular Probes) for 20 min at room temperature. After two washes, the cells were resuspended in imaging buffer (1% human serum albumin, 1 mM $CaCl_2$, 2 mM $MgCl_2$) and viewed using an LSM 510 microscope (Zeiss Microimaging). Quantification of nuclear localization was performed using the NIH ImageJ software package (colocalization plugin).

Data analysis

Fluorescent images were analyzed using MetaMorph (Molecular Devices), and the 340/380 ratio is displayed on a pseudocolor scale, with calculations done on randomly selected cells. SDs were calculated by measuring the sy.x value, the SD of the vertical distances of the data points from the regression line (GraphPad Prism; GraphPad). The linear regression line was fit using the 20- to 50-min time point data. The T cell displacement was measured using Volocity (Improvision) by tracking the movement of the center of fura 2 fluorescence (340:380 ratio). Only cells with tracks longer then 10 min were used in the analysis. To determine statistical significance, data were analyzed using one-way ANOVA (GraphPad).

Results

Single-cell calcium measurements

Hemoglobin-reactive $CD4^+$ T cells were isolated from the spleens of 2.102 TCR-transgenic mice and polarized to Th1, Th2, or Th17 cells in vitro. The 2.102 T cells respond vigorously to murine hemoglobin, are specific for Hb (64–76)/I-E^k, and have been used in previous studies examining altered peptide ligands, alloreactivity, and calcium signaling (34, 42–46). Intracellular cytokine staining confirmed proper polarization to the desired Th cell subtype by measuring their signature cytokines IFN-γ, IL-4, and IL-17 and representative histograms for each T cell subtype are shown (Fig. 1).

Calcium mobilization of the polarized Th1, Th2, and Th17 cells was visualized by loading the T cells with fura 2 and adding equal numbers of T cells to a monolayer of DCEK/ICAM APCs (Hi7-E^k) pulsed with 1 μM Hb (64–76) peptide overnight. None of the T cell subtypes showed evidence of calcium signaling when non-peptide-pulsed APC controls were used and a representative experiment using Th17 cells is shown (Fig. 2). The histograms show the plateau 340/380 ratio of each T cell in the field 10 min after T cells were loaded, and the percentage of T cells is shown at each ratio level. As shown in Fig. 2*A*, the majority of T cells remained at basal levels without addition of the hemoglobin peptide. Over 84% of the T cells interacting with APCs that had not been loaded with peptide had a 340/380 ratio below 2. In contrast, the addition of 1 μM Hb (64–76) peptide results in a $[Ca^{2+}]_i$ response, in which the majority of T cells are above the basal levels seen without the addition of peptide (Fig. 2*B*). The background $[Ca^{2+}]_i$ levels and necessity of a stimulatory peptide for T cell $[Ca^{2+}]_I$ induction were the same for Th1 and Th2 cells (data not shown). These data demonstrate the sensitivity and quantitative nature of the live cell imaging assay, which allows for the characterization of differences in T cell $[Ca^{2+}]_i$ signaling.

The $[Ca^{2+}]_i$ levels for all three T cell types were first visualized on a population level, providing a broad view of each T cell subtype $[Ca^{2+}]_i$ behavior. $[Ca^{2+}]_i$ profiles for each Th cell type were collected over 50 min and quantified using the 340/380 ratio. Five snapshots of the $[Ca^{2+}]_i$ intensity profiles (5, 15, 25, 35, and 45 min) are shown as each of the three Th subsets interacts with Hb (64–76) peptide-loaded APCs (1 μM) (Fig. 3*A*). The single-cell and statistical analysis are discussed below, but in these snapshots one can observe qualitatively that Th1 cells have the highest sustained levels of Ca^{2+} mobilization over time, Th2 have the lowest sustained Ca^{2+} levels, and Th17 cells have intermediate Ca^{2+} levels (Fig. 3*A*).

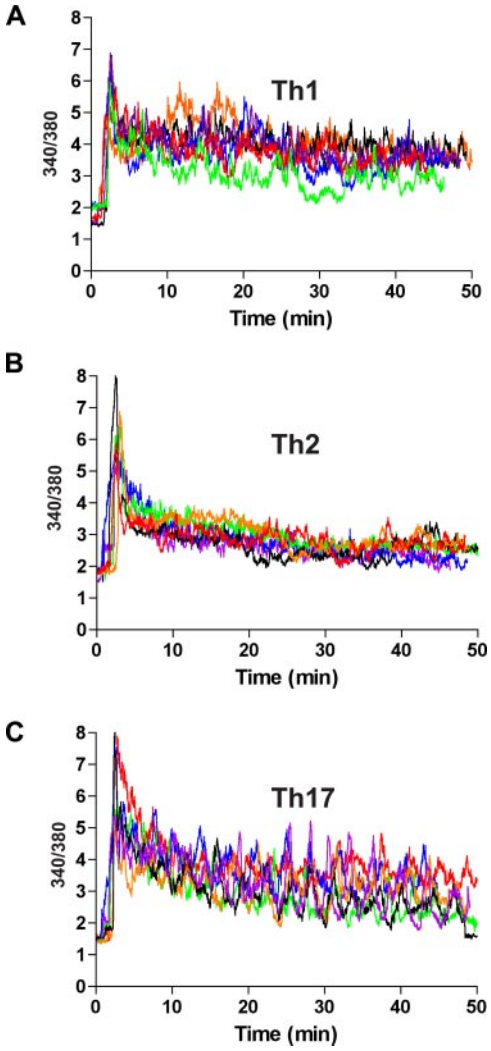

FIGURE 4. Overlay of six representative Th1, Th2, and Th17 $[Ca^{2+}]_i$ profiles taken from five different imaging experiments (1 μM Hb peptide). *A*, Overlay of six representative Th1 cell $[Ca^{2+}]_i$ profiles. Th1 cells have a high initial spike, followed by sustained $[Ca^{2+}]_i$ levels that oscillate numerous times. *B*, Overlay of six representative Th2 cell $[Ca^{2+}]_i$ profiles. Th2 cells have a high initial spike, followed by a rapid decrease with few oscillations. *C*, Overlay of six representative Th1 cell $[Ca^{2+}]_i$ profiles. Th17 cells have an initial high spike, followed by sustained $[Ca^{2+}]_i$ levels that are intermediate between Th1 and Th2 levels and oscillations that are similar to Th1 cells and more numerous than Th2 cells.

The T cell plateau $[Ca^{2+}]_i$ levels from this experiment were quantified at the 5-min time point, and the histograms show the percentage of T cells at their corresponding 340/380 levels (Fig. 3*B*). Th2 cells are found more predominantly at lower levels (mean $\pm$ SEM = 3.064 $\pm$ 0.1146) than Th1 cells (4.268 $\pm$ 0.1165), and this pattern of Th1 cells having higher plateau $[Ca^{2+}]_i$ levels than Th2 cells is consistent with studies published previously (32, 34). Th17 cell plateau $[Ca^{2+}]_i$ levels (4.066 $\pm$ 0.1363) are also significantly higher than Th2 cells, and Th17 cells have a similar mean and distribution as Th1 cells at the 5-min time point.

Th17 cells have a distinct calcium profile

Single-cell analysis of $[Ca^{2+}]_i$ for each Th subtype was performed in five separate experiments (45 T cells from each subtype were

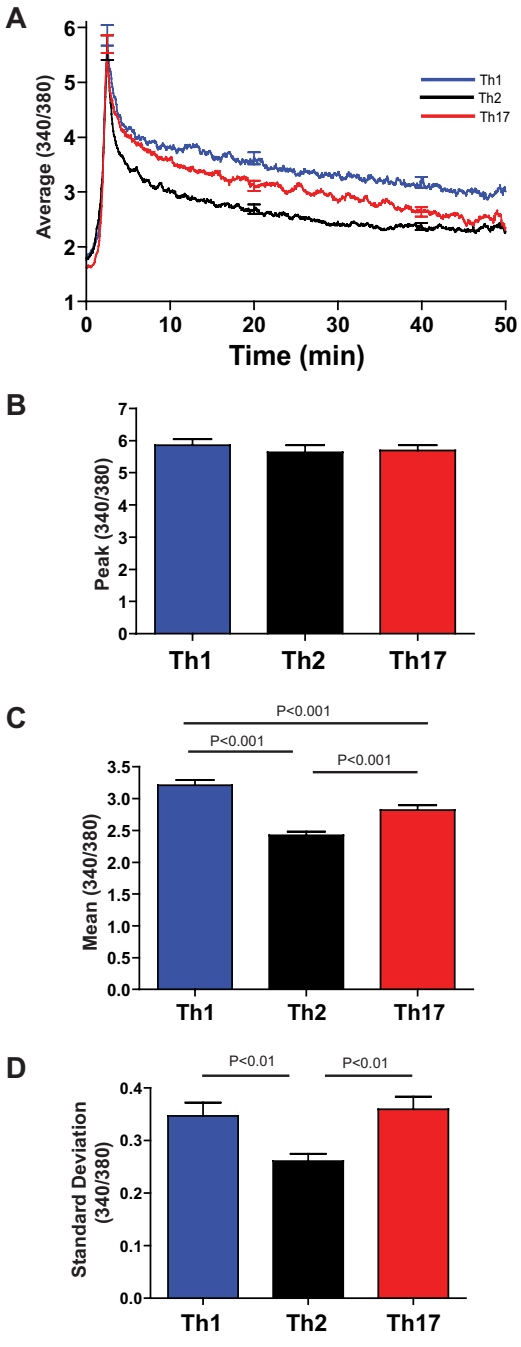

FIGURE 5. Average Th1, Th2, and Th17 $[Ca^{2+}]_i$ profile and statistical analysis of the peak, mean, and oscillatory values. *A*, Curves showing the average $[Ca^{2+}]_i$ mobilization (340/380 ratio) value at each time point over a 50-min time span ($n = 45$). Error bars show the SE at the influx peak, 20-min, and 40-min time points, and are omitted elsewhere for clarity. *B*, Statistical comparison of the peak $[Ca^{2+}]_i$ levels (340/380 ratios) for Th1, Th2, and Th17 cells. *C*, Statistical comparison of the sustained $[Ca^{2+}]_i$ levels (340/380 ratios) after the initial peak (mean from the 20- to 50-min window). *D*, Statistical analysis of SD (oscillations) upon linear regression analysis of each group (20- to 50-min window) (58).

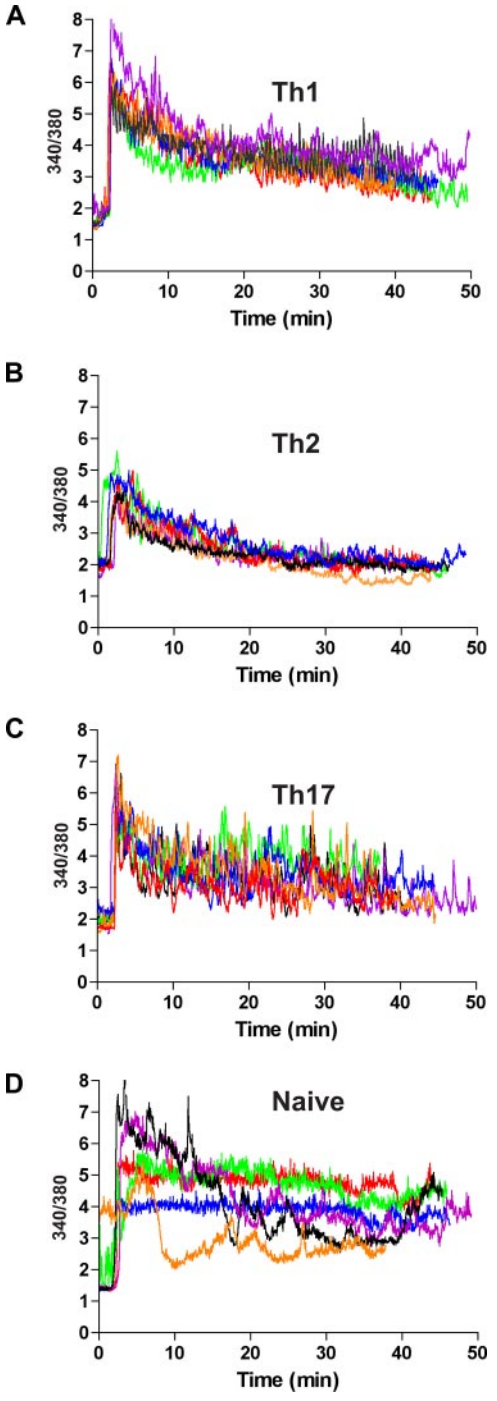

FIGURE 6. Overlay of six representative Th1, Th2, Th17, and naive T cell $[Ca^{2+}]_i$ profiles (0.1 μM Hb peptide). *A*, Overlay of six representative Th1 cell $[Ca^{2+}]_i$ profiles. Th1 cells have a high initial spike, followed by sustained $[Ca^{2+}]_i$ levels that oscillate numerous times. *B*, Overlay of six representative Th2 cell $[Ca^{2+}]_i$ profiles. Th2 cells have a high initial spike, followed by a rapid decrease with few oscillations. *C*, Overlay of six representative Th17 cell $[Ca^{2+}]_i$ profiles. Th17 cells have an initial high spike, followed by sustained $[Ca^{2+}]_i$ levels that oscillate numerous times. *D*, Overlay of six representative naive cell $[Ca^{2+}]_i$ profiles. These naive T cells ($CD4^+$, $CD62L^{high}$, $CD44^{low}$) have an initial high spike, followed by sustained $[Ca^{2+}]_i$ levels that oscillate numerous times.

measured) to obtain a global representation of the phenotype induced. An overlay of six representative profiles for each T cell subtype is shown to illustrate the characteristics of their different $[Ca^{2+}]_i$ patterns (Fig. 4). These traces show the $[Ca^{2+}]_i$ levels over 50 min while the T cells are interacting with the stimulatory Hb (64–76) peptide presented by APCs. Th1 cells have a high initial spike of $[Ca^{2+}]_i$, followed by high sustained $[Ca^{2+}]_i$ levels that oscillate numerous times (Fig. 4*A*). Th2 cells also have a high initial spike of $[Ca^{2+}]_i$, followed by a more rapid decrease with few oscillations (Fig. 4*B*). Th17 cells also have an initial high spike of $[Ca^{2+}]_i$, followed by sustained $[Ca^{2+}]_i$ levels that are

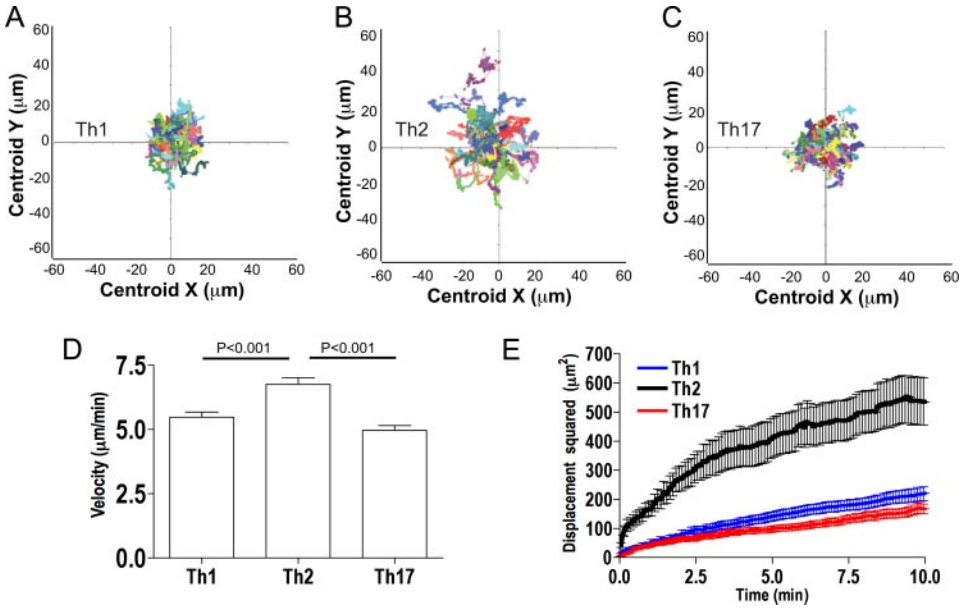

FIGURE 7. In vitro motility analysis of Th1, Th2, and Th17 cells. *A–C*, Flower plots showing representative Th1, Th2, and Th17 displacement tracks over 50 min. *D*, Histogram showing the mean velocities (μm/min) for Th1, Th2, and Th17 cells from five separate experiments (n = 254 Th1, 130 Th2, 202 Th17). *E*, Motility analysis of Th1, Th2, and Th17 cells examining displacement squared (μm^2) over a 10-min time span from five separate experiments (n = 254 Th1, 130 Th2, 202 Th17). Th1 and Th17 cell displacement (μm^2) values were significantly lower than Th2 cells at all of the time points ($p < 0.001$).

intermediate between Th1 and Th2 levels and oscillations that are similar to Th1 cells and larger and more numerous than Th2 cells (Fig. 4*C*).

The average $[Ca^{2+}]_i$ profile, combining the 45 measurements from five separate experiments for each Th cell subtype at every time point, is shown to illustrate the $[Ca^{2+}]_i$ similarities and differences between the Th cell subtypes (Fig. 5*A*). Upon stimulation by Ag, the populations of all three of the T cell subtypes have statistically identical $[Ca^{2+}]_i$ peaks (Fig. 5*B*). After the initial spike of $[Ca^{2+}]_i$, Th1 cells maintain the highest level of sustained $[Ca^{2+}]_i$, Th17 cells are intermediate, and Th2 cells have the lowest sustained $[Ca^{2+}]_i$ levels. Error bars show the SEM at the influx peak and at the 20- and 40-min time points; the error bars are omitted elsewhere for clarity.

Statistical analysis of the mean of the sustained $[Ca^{2+}]_i$ levels after the initial $[Ca^{2+}]_i$ peak revealed significant differences between T cell subtypes. Th1 cells have significantly higher mean $[Ca^{2+}]_i$ levels than Th17 cells during the 20- to 50-min time period after Ag stimulation, and Th17 cells have significantly higher levels than Th2 cells during this same time (Fig. 5*C*). There are also significant differences in $[Ca^{2+}]_i$ oscillations between T cell subtypes during the 20- to 50-min time period. Our experiments showed consistent $[Ca^{2+}]_i$ oscillation differences between the Th1 and Th2 cell subtypes, supportive of the previously published $[Ca^{2+}]_i$ profiles (34), as well as highlighting that Th17 cells have $[Ca^{2+}]_i$ oscillation levels that are similar to Th1 cells and significantly greater than Th2 cells (Fig. 5*D*). Thus, these data identify a distinct $[Ca^{2+}]_i$ profile for Th17 cells compared with Th1 and Th2 cells. Th17 cells have similar peak levels initially, but have intermediate sustained $[Ca^{2+}]_i$ levels and oscillation levels similar to Th1 cells and significantly higher than Th2 cells.

The previous experiments (Figs. 4 and 5) were performed using 1 μM Hb (64–76) peptide, which causes maximal 2.102 T cell proliferation. We also examined 2.102 T cells to see whether they responded similarly to 0.1 μM Hb (64–76) peptide, a 10-fold lower peptide concentration that causes a submaximal proliferation response in 2.102 T cells (34). Single-cell analysis of $[Ca^{2+}]_i$ for each Th subtype was performed, and an overlay of six representative profiles for each T cell subtype is shown (Fig. 6, *A–C*). Using this lower peptide concentration, as was seen with 1 μM Hb (64–76), the Th1 cells have high sustained $[Ca^{2+}]_i$ levels that oscillate numerous times (Fig. 6*A*). Th2 cells have lower sustained $[Ca^{2+}]_i$ levels and fewer oscillations (Fig. 6*B*), and Th17 cells have higher sustained $[Ca^{2+}]_i$ levels and more numerous oscillations (Fig. 6*C*). Thus, the calcium profiles are similar at two peptide concentrations that result in different levels of proliferation.

To determine the $[Ca^{2+}]_i$ profile of naive T cells, we enriched for splenic $CD4^+$ T cells and then sorted for a population of $CD4^+$, $CD62L^{high}$, $CD44^{low}$ T cells. Single-cell analysis of $[Ca^{2+}]_i$ for these sorted naive T cells was performed, and an overlay of six representative profiles is shown (Fig. 6*D*). The naive 2.102 T cells $[Ca^{2+}]_i$ profile is more similar to Th1 and Th17 cells than Th2 with a higher sustained level of $[Ca^{2+}]_i$ and more oscillations, suggesting that the Th2 cells lose the ability to engage this pathway as they mature (34).

Th17 cells have similar in vitro motility as Th1 cells

Because we have observed significant differences in $[Ca^{2+}]_i$ levels and oscillations between T cell subsets, we examined T cell motility to see whether these differences were substantial enough to cause functional differences. $[Ca^{2+}]_i$ signaling has been shown to play an important role in lymphocyte motility, with studies examining cellular motility showing that elevated levels of $[Ca^{2+}]_i$ correlate with inhibited T cell motility (31, 35–37). Based on the $[Ca^{2+}]_i$ profiles of the T cell subtypes, $[Ca^{2+}]_i$ means of Th1>Th17>Th2, and Th1 and Th17 cells with increased oscillations compared with Th2 cells (Fig. 5), we predicted that Th1 cells would be the least motile, Th2 the most, and Th17 cells similar to Th1 cells. To quantify this, we measured the motility of the Th cell populations as they interacted with APCs in vitro.

The distance traveled (displacement) for Th1, Th2, and Th17 cells was measured in five experiments, and the cell tracks were normalized to their starting coordinates. Representative plots are shown for Th1 (Fig. 7*A*), Th2 (Fig. 7*B*), and Th17 cells (Fig. 7*C*). Cell velocities for these cells were also measured, and the mean values for Th1 and Th17 cells were significantly lower than Th2 cells (Fig. 7*D*). Motility analysis, examining displacement squared (μm^2) for 10 min, revealed that Th1 and Th17 cells exhibit similar behavior and both are significantly less motile than Th2 cells ($p < 0.001$) (Fig. 7*E*). The addition of ionomycin to Th2 cells resulted in a 2- to 3-fold decrease in Th2 cell motility (data not shown). Thus, the higher $[Ca^{2+}]_i$ levels in Th17 and Th1 cells correlated

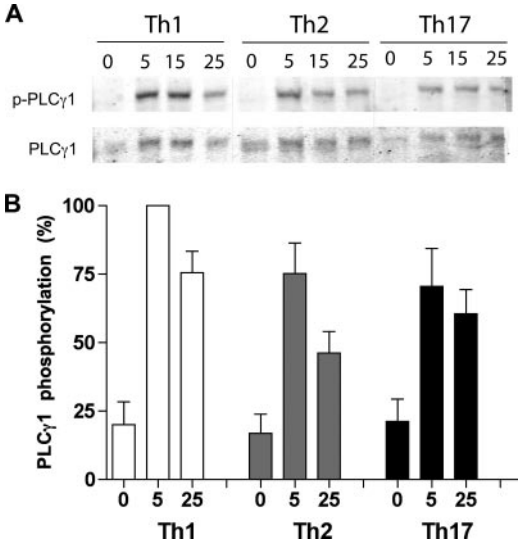

FIGURE 8. Western blot analysis of Th cell PLCγ1 phosphorylation. *A*, Representative PLCγ1 Western blot. Phosphorylated and nonphosphorylated bands for Th1, Th2, and Th17 cells at four time points (0, 5, 15, and 25 min). *B*, Quantification of PLCγ1 phosphorylation. At the 25-min time point, there is a trend toward Th1>Th17>Th2, but there is not a statistically significant difference among Th1, Th2, and Th17 cells at any of the time points. These data are from three separate experiments; the 15-min time point is not included in the quantification because it was only done once.

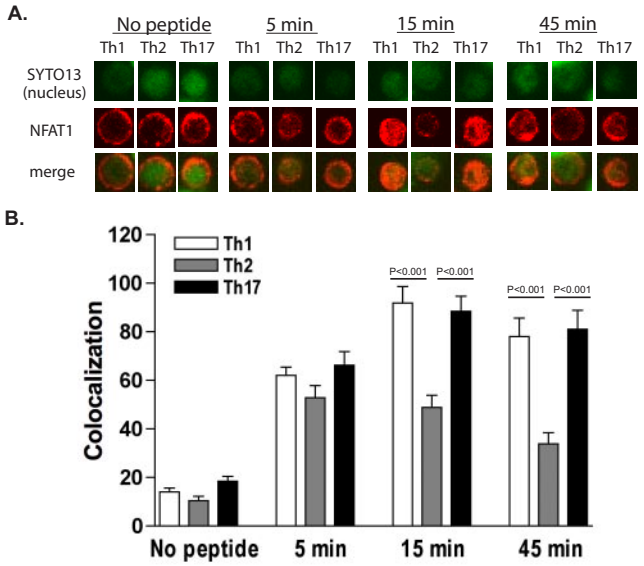

FIGURE 9. NF-AT nuclear localization in Th cells. *A*, Representative cells (Th1, Th2, and Th17) at no peptide, 5-min, 15-min, and 45-min time points. *Top panels*, The nuclei were stained with SYTO13 (green); *middle panels*, NF-AT1 (red) nuclear localization was measured; and *bottom panels*, show the merge of the two. *B*, Quantification of colocalization of NF-AT in the nucleus. Th2 cell colocalization levels are significantly lower ($p < 0.001$) than Th1 and Th17 cell levels at the 15- and 45-min time points. These data are representative of a total of 30 cells/sample taken from three independent experiments.

with lower motility compared with the Th2 cells that have lower $[Ca^{2+}]_i$ levels.

Th cell PLCγ1 expression levels similar

To understand the mechanism of these $[Ca^{2+}]_i$ differences, we examined PLCγ1 phosphorylation levels by Western blot. PLCγ1 plays a critical role in the generation of the second messengers 1,4,5-triphosphate and diacylglycerol, which trigger calcium release from intracellular Ca^{2+} stores (47). T cells were stimulated at time points ranging from 0 to 25 min (Fig. 8*A*), and the phosphorylated and nonphosphorylated levels of PLCγ1 were quantified (Fig. 8*B*). At the 25-min time point, there appears to be a trend of Th1>Th17>Th2, but when examining three independent experiments there is not a statistically significant difference between the samples at any time point. Although it is possible that this difference is biologically meaningful, the data are not conclusive. We also looked at overall tyrosine phosphorylation and were unable to see any dramatic differences between the samples that might be responsible for the $[Ca^{2+}]_i$ differences (data not shown).

NF-AT nuclear localization levels significantly different

To examine whether the $[Ca^{2+}]_i$ differences measured have a downstream effect, we analyzed the nuclear localization of NF-AT for each T cell subtype over multiple time points (Fig. 9*A*). Nuclear localization was quantified (Fig. 9*B*) for each Th cell (30 cells/sample from three independent experiments) and time point (0, 5, 15, and 45 min). At the 0- and 5-min time points, there is no significant difference between T cell subtypes, but at the 15- and 45-min time points the Th1 and Th17 T cells have significantly higher levels ($p < 0.001$) of NF-AT nuclear localization compared with Th2 cells. Thus, initially NF-AT levels are identical between T cell subtypes, but by 15 min there is a significant difference. The $[Ca^{2+}]_i$ differences we have seen in these cells have a similar pattern to NF-AT nuclear localization, with initial $[Ca^{2+}]_i$ levels identical and then mean and oscillatory levels different (Figs. 4 and 5), suggesting that the NF-AT differences may be due in part to the divergent $[Ca^{2+}]_i$ patterns.

Discussion

In this study, we provide for the first time an analysis of the $[Ca^{2+}]_i$ signaling profile of the recently identified Th17 cells in comparison with Th1 and Th2 cells. Because Th17 cells exhibit a distinct functional response (IL-17 secretion) from Th1 and Th2 cells, we hypothesized that Th17 cells would exhibit a unique $[Ca^{2+}]_i$ signaling pattern. Our study found that Th17 cells do have a $[Ca^{2+}]_i$ signaling pattern that is distinctive from Th1 and Th2 cells (Fig. 4). Th17 cells have sustained $[Ca^{2+}]_i$ levels that are intermediate between Th1 and Th2 cells, and also have high levels of oscillations similar to Th1 cells and significantly greater than Th2 cells (Fig. 5).

Elevation of $[Ca^{2+}]_i$ is a key T cell activation signal, and the amplitude, duration, and kinetics of this signal help instruct lymphocyte responses to Ag stimulation (30, 48). Studies have reported a variety of T cell $[Ca^{2+}]_i$ responses ranging from transients, repetitive oscillations, and sustained elevations from 200 nM to over 1 μM (34, 37, 49–51). The $[Ca^{2+}]_i$ signal is not a binary switch, but able to transmit signaling information by multiple parameters (30). Different duration and patterns of sustained $[Ca^{2+}]_i$ levels can vary transcription factor activity and the subsequent genes that are transcribed. For example, studies using B cells have shown that the transcriptional factors NF-κB, JNK, and NF-AT are all differentially regulated by the amplitude and duration of the $[Ca^{2+}]_i$. NF-κB and JNK are preferentially activated by a large transient $[Ca^{2+}]_i$ rise (low calcium sensitivity with activation resulting in sustained activity), whereas NF-AT is selectively activated by a low sustained plateau (higher calcium sensitivity that is rapidly reversible upon decreases in calcium levels) (30,

52). Different $[Ca^{2+}]_i$ levels may also optimize cytokine production by changing histone acetylation during polarization or induction of specific isoforms of transcription factors (53–55).

Sustained $[Ca^{2+}]_i$ levels of ~200–500 nM are sufficient for thymocyte immobilization, positive selection, and NF-AT translocation (27, 31). According to our estimates, a 340/380 ratio of 3 in our experiments is equal to ~300 nM $[Ca^{2+}]_i$. Thus, Th1 cells in our experiments on average maintain $[Ca^{2+}]_i$ levels at or above this level for ~45 min, whereas Th2 cells drop below this level on average after ~10 min, and Th17 cells maintain this level for ~25 min. Thus, Th cell subsets have dramatically different time intervals of biologically relevant $[Ca^{2+}]_i$ levels (Fig. 5*A*).

The $[Ca^{2+}]_i$ oscillation differences, Th1 and Th17 cells significantly greater than Th2 cells, could affect T cell behavior in numerous ways ranging from development, gene transcription, and motility. $[Ca^{2+}]_i$ oscillations have also been shown to optimize T cell sensitivity to stimuli and enhance the efficiency and specificity of signaling, resulting in preferential expression of genes and associated cellular responses (56–59). The physiological relevance of $[Ca^{2+}]_i$ oscillations has been examined using Jurkat T cells and rat basophilic leukemia cells (59, 60). Of interest, both studies found that at low levels of stimulation, $[Ca^{2+}]_i$ oscillations more efficiently activate NF-AT than a sustained $[Ca^{2+}]_i$ increase.

To evaluate the possible downstream effects of the calcium differences we have seen on gene transcription, we measured NF-AT localization of these T cells at various time points (Fig. 9). We found that Th1 and Th17 cells have significantly higher levels of NF-AT nuclear localization compared with Th2 cells at the 15- and 45-min time points measured. This correlates generally with our calcium measurements where we did not see significant differences initially, but a few minutes after the peak the calcium levels are significantly different (Fig. 5*A*). The idea that the higher sustained levels of calcium and increased oscillations measured in Th1 and Th17 cells increase NF-AT localization compared with Th2 cells is consistent with other studies that have examined the relationship between NF-AT and calcium (56). The exact role of NF-AT and NF-κB in the process of IL-17 production is still uncertain. Previous studies have reported that human IL-17 has two NF-AT promotor elements and that the murine IL-17 pathway is sensitive to cyclosporin A and MAPK inhibitors, suggesting the involvement of calcineurin/NF-AT and MAPK signaling pathways (61–64).

A strong correlation between increases in T cell $[Ca^{2+}]_i$ levels and decreased T cell and thymocyte motility has been observed (35). Engagement of a stimulatory ligand results in elevation of $[Ca^{2+}]_i$ levels and generation of a long-lived stop signal, permitting (or as a result of) increased interactions between the T cell and APCs (36). More recently, using two-photon microscopy, T cell $[Ca^{2+}]_i$ oscillations have been reported to regulate thymocyte motility and positive selection. Naive thymocytes were shown to be highly mobile at low $[Ca^{2+}]_i$ levels and immobile upon sustained $[Ca^{2+}]_i$ oscillations, permitting stationary contacts with peptide MHC-bearing cells (31). Our motility analysis of the Th1, Th2, and Th17 cells revealed that Th17 cells are similar to Th1 cells in their velocity and displacement and significantly greater than Th2 cells (Fig. 7). The Th17 cells $[Ca^{2+}]_i$ profile is more like Th1 cells than Th2 cells. Th17 cells have significantly more oscillations than Th2 cells and intermediate levels of sustained $[Ca^{2+}]_i$ (Figs. 4 and 5). These data are consistent with the previous findings of higher levels of $[Ca^{2+}]_i$ signaling causing decreased motility (35, 65).

To understand the mechanism of these $[Ca^{2+}]$ differences, we examined PLCγ1 expression levels (Fig. 8) and overall phosphotyrosine levels (data not shown). We focused on PLCγ1 phosphorylation because it plays a critical role in the pathway that leads to activation of the calcium release-activated Ca^{2+} channel and the influx of extracellular Ca^{2+} (47, 66). Our analysis did not reveal any dramatic differences in overall phosphotyrosine or PLCγ1 phosphorylation levels. There was a trend (Th1>Th17>Th2) at the 25-min time point of PLCγ1 analysis, and it is possible that this is biologically important, but it was not statistically significant. It is likely that the mechanism for calcium differences we have seen involves multiple signaling players, but to date it has not been definitively determined.

Our study in this work has described for the first time the characterization of the Th17 $[Ca^{2+}]_i$ signaling pathway, which is unique from Th1 and Th2 cells, and the analysis of Th17 cell motility behavior, which is similar to Th1 cells and significantly less motile than Th2 cells. Although PLCγ1 phosphorylation levels were not significantly different, our analysis revealed that NF-AT nuclear localization was significantly higher in Th1 and Th17 cells at later time points compared with Th2 cells. Understanding of the Th17 $[Ca^{2+}]_i$ signaling pathway and its functional differences enhances our understanding of how Th17 cells respond differently to pathogens and are involved in inflammatory-related disease. Thus, the dissection of the Th17 $[Ca^{2+}]_i$ pathway provides insights into what we currently know about Th17 cells and should prompt further investigation into the role of $[Ca^{2+}]_i$ and Th cell function.

Acknowledgments

We thank Henry Kao and S. Celeste Morley for critically reading the manuscript, Jennifer N. Lynch and Bernd H. Zinselmeyer for help with the motility analysis, and the members of the Allen laboratory for their valuable comments.

Disclosures

The authors have no financial conflict of interests.

References

1. Mosmann, T. R., H. Cherwinski, M. W. Bond, M. A. Giedlin, and R. L. Coffman. 1986. Two types of murine helper T cell clone. I. Definition according to profiles of lymphokine activities and secreted proteins. *J. Immunol.* 136: 2348–2357.
2. Abbas, A. K., K. M. Murphy, and A. Sher. 1996. Functional diversity of helper T lymphocytes. *Nature* 383: 787–793.
3. Coffman, R. L. 2006. Origins of the T_H1–T_H2 model: a personal perspective. *Nat. Immunol.* 7: 539–541.
4. Mosmann, T. R., and R. L. Coffman. 1989. TH1 and TH2 cells: different patterns of lymphokine secretion lead to different functional properties. *Annu. Rev. Immunol.* 7: 145–173.
5. Hsieh, C. S., S. E. Macatonia, C. S. Tripp, S. F. Wolf, A. O'Garra, and K. M. Murphy. 1993. Development of TH1 $CD4^+$ T cells through IL-12 produced by *Listeria*-induced macrophages. *Science* 260: 547–549.
6. Shinkai, K., M. Mohrs, and R. M. Locksley. 2002. Helper T cells regulate type-2 innate immunity in vivo. *Nature* 420: 825–829.
7. Infante-Duarte, C., H. F. Horton, M. C. Byrne, and T. Kamradt. 2000. Microbial lipopeptides induce the production of IL-17 in Th cells. *J. Immunol.* 165: 6107–6115.
8. Bettelli, E., M. Oukka, and V. K. Kuchroo. 2007. T_H-17 cells in the circle of immunity and autoimmunity. *Nat. Immunol.* 8: 345–350.
9. Veldhoen, M., R. J. Hocking, C. J. Atkins, R. M. Locksley, and B. Stockinger. 2006. TGFβ in the context of an inflammatory cytokine milieu supports de novo differentiation of IL-17-producing T cells. *Immunity* 24: 179–189.
10. Stockinger, B., and M. Veldhoen. 2007. Differentiation and function of Th17 T cells. *Curr. Opin. Immunol.* 19: 281–286.
11. Park, H., Z. Li, X. O. Yang, S. H. Chang, R. Nurieva, Y. H. Wang, Y. Wang, L. Hood, Z. Zhu, Q. Tian, and C. Dong. 2005. A distinct lineage of CD4 T cells regulates tissue inflammation by producing interleukin 17. *Nat. Immunol.* 6: 1133–1141.
12. Weaver, C. T., L. E. Harrington, P. R. Mangan, M. Gavrieli, and K. M. Murphy. 2006. Th17: an effector CD4 T cell lineage with regulatory T cell ties. *Immunity* 24: 677–688.
13. Harrington, L. E., R. D. Hatton, P. R. Mangan, H. Turner, T. L. Murphy, K. M. Murphy, and C. T. Weaver. 2005. Interleukin 17-producing $CD4^+$ effector T cells develop via a lineage distinct from the T helper type 1 and 2 lineages. *Nat. Immunol.* 6: 1123–1132.
14. Steinman, L. 2007. A brief history of T_H17, the first major revision in the T_H1/T_H2 hypothesis of T cell-mediated tissue damage. *Nat. Med.* 13: 139–145.
15. Weaver, C. T., R. D. Hatton, P. R. Mangan, and L. E. Harrington. 2007. IL-17 family cytokines and the expanding diversity of effector T cell lineages. *Annu. Rev. Immunol.* 25: 821–852.

16. Cua, D. J., J. Sherlock, Y. Chen, C. A. Murphy, B. Joyce, B. Seymour, L. Lucian, W. To, S. Kwan, T. Churakova, et al. 2003. Interleukin-23 rather than interleukin-12 is the critical cytokine for autoimmune inflammation of the brain. *Nature* 421: 744–748.
17. Nakae, S., A. Nambu, K. Sudo, and Y. Iwakura. 2003. Suppression of immune induction of collagen-induced arthritis in IL-17-deficient mice. *J. Immunol.* 171: 6173–6177.
18. Hue, S., P. Ahern, S. Buonocore, M. C. Kullberg, D. J. Cua, B. S. McKenzie, F. Powrie, and K. J. Maloy. 2006. Interleukin-23 drives innate and T cell-mediated intestinal inflammation. *J. Exp. Med.* 203: 2473–2483.
19. Zheng, Y., D. M. Danilenko, P. Valdez, I. Kasman, J. Eastham-Anderson, J. Wu, and W. Ouyang. 2007. Interleukin-22, a T_H17 cytokine, mediates IL-23-induced dermal inflammation and acanthosis. *Nature* 445: 648–651.
20. Langrish, C. L., Y. Chen, W. M. Blumenschein, J. Mattson, B. Basham, J. D. Sedgwick, T. McClanahan, R. A. Kastelein, and D. J. Cua. 2005. IL-23 drives a pathogenic T cell population that induces autoimmune inflammation. *J. Exp. Med.* 201: 233–240.
21. Fossiez, F., J. Banchereau, R. Murray, C. Van Kooten, P. Garrone, and S. Lebecque. 1998. Interleukin-17. *Int. Rev. Immunol.* 16: 541–551.
22. Gor, D. O., N. R. Rose, and N. S. Greenspan. 2003. TH1–TH2: a procrustean paradigm. *Nat. Immunol.* 4: 503–505.
23. Liew, F. Y. 2002. T_H1 and T_H2 cells: a historical perspective. *Nat. Rev. Immunol.* 2: 55–60.
24. McKenzie, B. S., R. A. Kastelein, and D. J. Cua. 2006. Understanding the IL-23-IL-17 immune pathway. *Trends Immunol.* 27: 17–23.
25. Augustine, G. J., F. Santamaria, and K. Tanaka. 2003. Local calcium signaling in neurons. *Neuron* 40: 331–346.
26. Berridge, M. J. 2005. Unlocking the secrets of cell signaling. *Annu. Rev. Physiol.* 67: 1–21.
27. Gallo, E. M., K. Cante-Barrett, and G. R. Crabtree. 2006. Lymphocyte calcium signaling from membrane to nucleus. *Nat. Immunol.* 7: 25–32.
28. Berridge, M. J., M. D. Bootman, and P. Lipp. 1998. Calcium: a life and death signal. *Nature* 395: 645–648.
29. Randriamampita, C., and A. Trautmann. 2004. Ca^{2+} signals and T lymphocytes; "new mechanisms and functions in Ca^{2+} signalling." *Biol. Cell* 96: 69–78.
30. Lewis, R. S. 2001. Calcium signaling mechanisms in T lymphocytes. *Annu. Rev. Immunol.* 19: 497–521.
31. Bhakta, N. R., D. Y. Oh, and R. S. Lewis. 2005. Calcium oscillations regulate thymocyte motility during positive selection in the three-dimensional thymic environment. *Nat. Immunol.* 6: 143–151.
32. Fanger, C. M., A. L. Neben, and M. D. Cahalan. 2000. Differential Ca^{2+} influx, KCa channel activity, and Ca^{2+} clearance distinguish Th1 and Th2 lymphocytes. *J. Immunol.* 164: 1153–1160.
33. Gajewski, T. F., S. R. Schell, and F. W. Fitch. 1990. Evidence implicating utilization of different T cell receptor-associated signaling pathways by TH1 and TH2 clones. *J. Immunol.* 144: 4110–4120.
34. Sloan-Lancaster, J., T. H. Steinberg, and P. M. Allen. 1997. Selective loss of the calcium ion signaling pathway in T cells maturing toward a T helper 2 phenotype. *J. Immunol.* 159: 1160–1168.
35. Negulescu, P. A., T. B. Krasieva, A. Khan, H. H. Kerschbaum, and M. D. Cahalan. 1996. Polarity of T cell shape, motility, and sensitivity to antigen. *Immunity* 4: 421–430.
36. Dustin, M. L., S. K. Bromley, Z. Kan, D. A. Peterson, and E. R. Unanue. 1997. Antigen receptor engagement delivers a stop signal to migrating T lymphocytes. *Proc. Natl. Acad. Sci. USA* 94: 3909–3913.
37. Donnadieu, E., G. Bismuth, and A. Trautmann. 1994. Antigen recognition by helper T cells elicits a sequence of distinct changes of their shape and intracellular calcium. *Curr. Biol.* 4: 584–595.
38. Randolph, D. A., G. Huang, C. J. Carruthers, L. E. Bromley, and D. D. Chaplin. 1999. The role of CCR7 in TH1 and TH2 cell localization and delivery of B cell help in vivo. *Science* 286: 2159–2162.
39. Grakoui, A., D. L. Donermeyer, O. Kanagawa, K. M. Murphy, and P. M. Allen. 1999. TCR-independent pathways mediate the effects of antigen dose and altered peptide ligands on Th cell polarization. *J. Immunol.* 162: 1923–1930.
40. Donermeyer, D. L., K. S. Weber, D. M. Kranz, and P. M. Allen. 2006. The study of high-affinity TCRs reveals duality in T cell recognition of antigen: specificity and degeneracy. *J. Immunol.* 177: 6911–6919.
41. Grynkiewicz, G., M. Poenie, and R. Y. Tsien. 1985. A new generation of Ca^{2+} indicators with greatly improved fluorescence properties. *J. Biol. Chem.* 260: 3440–3450.
42. Daniel, C., A. Grakoui, and P. M. Allen. 1998. Inhibition of an in vitro $CD4^+$ T cell alloresponse using altered peptide ligands. *J. Immunol.* 160: 3244–3250.
43. Daniel, C., S. Horvath, and P. M. Allen. 1998. A basis for alloreactivity: MHC helical residues broaden peptide recognition by the TCR. *Immunity* 8: 543–552.
44. Evavold, B. D., and P. M. Allen. 1991. Separation of IL-4 production from Th cell proliferation by an altered T cell receptor ligand. *Science* 252: 1308–1310.
45. Evavold, B. D., J. Sloan-Lancaster, and P. M. Allen. 1994. Antagonism of superantigen-stimulated helper T-cell clones and hybridomas by altered peptide ligand. *Proc. Natl. Acad. Sci. USA* 91: 2300–2304.
46. Felix, N. J., D. L. Donermeyer, S. Horvath, J. J. Walters, M. L. Gross, A. Suri, and P. M. Allen. 2007. Alloreactive T cells respond specifically to multiple distinct peptide-MHC complexes. *Nat. Immunol.* 8: 388–397.
47. Feske, S. 2007. Calcium signalling in lymphocyte activation and disease. *Nat. Rev. Immunol.* 7: 690–702.
48. Crabtree, G. R., and N. A. Clipstone. 1994. Signal transmission between the plasma membrane and nucleus of T lymphocytes. *Annu. Rev. Biochem.* 63: 1045–1083.
49. Freedman, B. D., Q. H. Liu, S. Somersan, M. I. Kotlikoff, and J. A. Punt. 1999. Receptor avidity and costimulation specify the intracellular Ca^{2+} signaling pattern in $CD4^+CD8^+$ thymocytes. *J. Exp. Med.* 190: 943–952.
50. Wulfing, C., J. D. Rabinowitz, C. Beeson, M. D. Sjaastad, H. M. McConnell, and M. M. Davis. 1997. Kinetics and extent of T cell activation as measured with the calcium signal. *J. Exp. Med.* 185: 1815–1825.
51. Negulescu, P. A., N. Shastri, and M. D. Cahalan. 1994. Intracellular calcium dependence of gene expression in single T lymphocytes. *Proc. Natl. Acad. Sci. USA* 91: 2873–2877.
52. Dolmetsch, R. E., R. S. Lewis, C. C. Goodnow, and J. I. Healy. 1997. Differential activation of transcription factors induced by Ca^{2+} response amplitude and duration. *Nature* 386: 855–858.
53. Avni, O., D. Lee, F. Macian, S. J. Szabo, L. H. Glimcher, and A. Rao. 2002. T_H cell differentiation is accompanied by dynamic changes in histone acetylation of cytokine genes. *Nat. Immunol.* 3: 643–651.
54. Hogan, P. G., L. Chen, J. Nardone, and A. Rao. 2003. Transcriptional regulation by calcium, calcineurin, and NFAT. *Genes Dev.* 17: 2205–2232.
55. Abbott, K. L., B. B. Friday, D. Thaloor, T. J. Murphy, and G. K. Pavlath. 1998. Activation and cellular localization of the cyclosporine A-sensitive transcription factor NF-AT in skeletal muscle cells. *Mol. Biol. Cell* 9: 2905–2916.
56. Lewis, R. S. 2003. Calcium oscillations in T-cells: mechanisms and consequences for gene expression. *Biochem. Soc. Trans.* 31: 925–929.
57. Utzny, C., M. Faroudi, and S. Valitutti. 2005. Frequency encoding of T-cell receptor engagement dynamics in calcium time series. *Biophys. J.* 88: 1–14.
58. Faroudi, M., C. Utzny, M. Salio, V. Cerundolo, M. Guiraud, S. Muller, and S. Valitutti. 2003. Lytic versus stimulatory synapse in cytotoxic T lymphocyte/target cell interaction: manifestation of a dual activation threshold. *Proc. Natl. Acad. Sci. USA* 100: 14145–14150.
59. Dolmetsch, R. E., K. Xu, and R. S. Lewis. 1998. Calcium oscillations increase the efficiency and specificity of gene expression. *Nature* 392: 933–936.
60. Li, W., J. Llopis, M. Whitney, G. Zlokarnik, and R. Y. Tsien. 1998. Cell-permeant caged InsP3 ester shows that Ca^{2+} spike frequency can optimize gene expression. *Nature* 392: 936–941.
61. Liu, X. K., X. Lin, and S. L. Gaffen. 2004. Crucial role for nuclear factor of activated T cells in T cell receptor-mediated regulation of human interleukin-17. *J. Biol. Chem.* 279: 52762–52771.
62. Liu, X. K., J. L. Clements, and S. L. Gaffen. 2005. Signaling through the murine T cell receptor induces IL-17 production in the absence of costimulation, IL-23 or dendritic cells. *Mol. Cell* 20: 339–347.
63. Cho, M. L., J. H. Ju, K. W. Kim, Y. M. Moon, S. Y. Lee, S. Y. Min, Y. G. Cho, H. S. Kim, K. S. Park, C. H. Yoon, et al. 2007. Cyclosporine A inhibits IL-15-induced IL-17 production in $CD4^+$ T cells via down-regulation of PI3K/Akt and NF-κB. *Immunol. Lett.* 108: 88–96.
64. Ziolkowska, M., A. Koc, G. Luszczykiewicz, K. Ksiezopolska-Pietrzak, E. Klimczak, H. Chwalinska-Sadowska, and W. Maslinski. 2000. High levels of IL-17 in rheumatoid arthritis patients: IL-15 triggers in vitro IL-17 production via cyclosporin A-sensitive mechanism. *J. Immunol.* 164: 2832–2838.
65. Wei, S. H., O. Safrina, Y. Yu, K. R. Garrod, M. D. Cahalan, and I. Parker. 2007. Ca^{2+} signals in $CD4^+$ T cells during early contacts with antigen-bearing dendritic cells in lymph node. *J. Immunol.* 179: 1586–1594.
66. Lucas, J. A., A. T. Miller, L. O. Atherly, and L. J. Berg. 2003. The role of Tec family kinases in T cell development and function. *Immunol. Rev.* 191: 119–138.